

1 **Alterations in bile acid metabolizing gut microbiota and specific bile**
2 **acid genes as a precision medicine to subclassify NAFLD**

3 **Short title: Bile acid metabolizing microbiota in NAFLD**

4 Na Jiao^{1,2,§}, Rohit Loomba^{3,§,*}, Zi-Huan Yang¹, Dingfeng Wu², Sa Fang², Richele
5 Bettencourt³, Ping Lan¹, Ruixin Zhu^{2,*}, Lixin Zhu^{1,4,*}

6

7 ¹ Guangdong Institute of Gastroenterology, Guangdong Provincial Key Laboratory of
8 Colorectal and Pelvic Floor Diseases, Department of Colorectal Surgery, the Sixth
9 Affiliated Hospital, Sun Yat-sen University, Guangzhou 510655, P.R. China.

10 ² Putuo people's Hospital, Department of Bioinformatics, Tongji University, Shanghai
11 200092, P.R.China.

12 ³ NAFLD Research Center, Division of Gastroenterology and Epidemiology,
13 Department of Medicine, University of California San Diego, La Jolla, California
14 92093, United States.

15 ⁴ Department of Biochemistry, Genome, Environment and Microbiome Community
16 of Excellence, The State University of New York at Buffalo, New York 14214,
17 United States.

18 § Equal contribution, * Corresponding authors

19

20 **Grant support:**

21 This work was supported by National Natural Science Foundation of China 81774152
22 (to RZ), 81770571 (to LZ), National Postdoctoral Program for Innovative Talents of
23 China BX20190393 (to NJ), China Postdoctoral Science Foundation 2019M663252
24 (to NJ) and 2019M651568 (to DW), Natural Science Foundation of Shanghai
25 16ZR1449800 (to RZ), Fundamental Research Funds for the Central Universities

26 19ykzd01(to LZ) and 20kypy07(to NJ), the Guangzhou Science and Technology Plan
27 Projects 201803040019 (to PL), Guangdong Province “Pearl River Talent Plan”
28 Innovation and Entrepreneurship Team Project (2019ZT08Y464 to LZ) and the
29 National Key Clinical Discipline of China, and Funds from the University at Buffalo
30 Community of Excellence in Genome, Environment and Microbiome (GEM) (to LZ).
31 RL receives funding support from NIEHS (5P42ES010337), NCATS
32 (5UL1TR001442), and NIDDK (R01DK106419). The funders had no role in study
33 design, data collection and analysis, decision to publish, or preparation of the
34 manuscript.

35 **Abbreviations:**

36 **baiA**, 3 α -hydroxysteroid dehydrogenase; **baiB**, bile acid-coenzyme A ligase; **baiCD**,
37 7 α -hydroxy-3-oxo-D4-cholenoic acid oxidoreductase; **baiE**, bile acid 7 α -
38 dehydratase; **baiF**, bile acid coenzyme A transferase/hydrolase; **baiG**, primary bile
39 acid transporter; **baiH**, 7beta-hydroxy-3-oxochol-24-oyl-CoA 4-desaturase; **baiI**, bile
40 acid 7beta-dehydratase; **BAs**, bile acids; **BSh**, bile salt hydrolase; **FXR**, farnesoid X
41 receptor; **HMM**, hidden Markov model; **HSDH**, hydroxysteroid dehydrogenase;
42 **MAG**, metagenome-assembled genome; **NAFLD**, non- alcoholic fatty liver disease;
43 **NASH**, non-alcoholic steatohepatitis; **WMS**, whole metagenome sequences.

44

45 **Corresponding authors:**

46 **Rohit Loomba (roloomba@ucsd.edu)**

47 NAFLD Research Center, Division of Gastroenterology and Epidemiology,
48 University of California San Diego, 9500 Gilman Drive, MC 0887, La Jolla, CA
49 92093, United States.

50 Tel: 1-858-246-2201

51 **Ruixin Zhu (rxzhu@tongji.edu.cn)**

52 Putuo people's Hospital, Department of Bioinformatics, Tongji University, 1239
53 Siping Road, Shanghai 200092, P.R. China.

54 Tel: 86-21-6598-1041

55 **Lixin Zhu (zhulx6@mail.sysu.edu.cn)**

56 Guangdong Institute of Gastroenterology, Guangdong Provincial Key Laboratory of

57 Colorectal and Pelvic Floor Diseases, Department of Colorectal Surgery, the Sixth

58 Affiliated Hospital, Sun Yat-sen University, Guangzhou 510655, P.R. China.

59 Tel: 86-199-46256235

60

61 **Disclosures:**

62 The authors have declared that no competing interests exist.

63 **Word count: 3216**

64

65 **Author's contributions:**

66 LZ, RL and RZ conceived and designed the project. Each author has contributed

67 significantly to the submitted work. NJ and RL drafted the manuscript. ZY, DW, SF,

68 RB, PL, RZ and LZ revised the manuscript. All authors read and approved the final

69 manuscript.

70

71 **Availability of data and materials:**

72 The datasets supporting the conclusions of this article are available in the NCBI's

73 Sequence Read Archive repository (<https://www.ncbi.nlm.nih.gov/bioproject/>),

74 under study accession number PRJNA373901, PRJNA420817, PRJEB1220 and

75 PRJEB6070.

76

77

78 **Synopsis**

79 The microbial markers identified at the species/strain levels may be useful for

80 non-invasive diagnosis of NAFLD. The microbial differences in bile acid metabolism

81 and strain-specific differences among NAFLD microbiota highlight the potential for

82 precision medicine in NAFLD treatment.

83

84

85

86 **Abstract**

87 **Background & Aims:** Multiple mechanisms for the gut microbiome contributing to

88 the pathogenesis of non-alcoholic fatty liver disease (NAFLD) have been implicated.

89 Here, we aim to investigate the contribution and potential application for altered bile

90 acid (BA) metabolizing microbe in NAFLD using whole metagenome sequencing

91 (WMS) data.

92 **Methods:** 86 well-characterized biopsy-proven NAFLD patients and 38 healthy

93 controls were included in the discovery cohort. Assembly-based analysis was

94 performed to identify BA-metabolizing microbes. Statistical tests, feature selection

95 and microbial interaction analysis were integrated to identify microbial alterations and

96 markers in NAFLD. An independent validation cohort was subjected to similar

97 analyses.

98 **Results:** NAFLD microbiota exhibited decreased diversity and microbial interactions.

99 We established a classifier model with 53 differential species exhibiting a robust

100 diagnostic accuracy (AUC=0.97) for detecting NAFLD. Next, 8 important

101 differential pathway markers including secondary BA biosynthesis were identified.

102 Specifically, increased abundance of 7 α -HSDH, baiA and baiB were detected in

103 NAFLD. Further, 10 of 50 BA-metabolizing metagenome-assembled genomes

104 (MAGs), from *Bacteroides ovatus* and *Eubacterium bifforme*, were dominant in

105 NAFLD and interplayed as a synergetic ecological guild. Importantly, two subtypes

106 of NAFLD patients were observed according to secondary BA metabolism potentials.

107 Elevated capability for secondary BA biosynthesis was also observed in the validation
108 cohort.

109 **Conclusions:** We identified novel bacterial BA-metabolizing genes and microbes that
110 may contribute to NAFLD pathogenesis and serve as disease markers. Microbial
111 differences in BA-metabolism and strain-specific differences among patients highlight
112 the potential for precision medicine in NAFLD treatment.

113 **Keywords:** NAFLD; gut microbiota; secondary BA synthesis; whole metagenome
114 sequencing data

115

116 **Introduction**

117 Non-alcoholic fatty liver disease(NAFLD) has become one of the leading causes of
118 liver disease worldwide, with the global prevalence estimated to be 24%.[1] NAFLD
119 is expected to be the No. 1 cause for cirrhosis in the United States within a decade.[2]

120 The pathogenic mechanism of NAFLD remains unclear. The current multiple-hit
121 hypothesis is that NAFLD is a consequence of a myriad of factors acting in a parallel
122 and synergistic manner in individuals with genetic predisposition.[3] Factors such as
123 insulin resistance, central obesity, environmental or nutritional factors, and gut
124 microbiota, as well as genetic and epigenetic factors, are linked to its pathogenesis.[2,
125 4, 5]

126 Recently, the crosstalk between the gut and the liver is increasingly recognized, and
127 many studies have reported dysregulated gut microbiota in NAFLD patients. [6-10]
128 There are several potential mechanisms for the gut microbiota to influence NAFLD
129 development. These effects are mediated by microbial components and metabolites,
130 such as lipopolysaccharide, alcohol, and bile acid(BA).[11]

131 BA not only facilitate the digestion and absorption of fatty foods as detergent, they
132 also act as important signaling molecules via nuclear receptors, such as farnesoid X
133 receptor(FXR) and G protein coupled BA receptor(GPBAR1 or TGR5) to modulate
134 hepatic BA synthesis, glucose and lipid metabolism. Recently, we observed
135 suppressed BA-mediated FXR signaling in NAFLD liver and intestine, which is in
136 harmony with increased secondary BA production. Furthermore, using 16S rRNA

137 data, we observed elevated abundance of secondary BA metabolizing related bacteria
138 and pathways in the gut microbiome of NAFLD. [12] However, the 16S rRNA
139 sequencing data has limited resolution which does not allow the identification of the
140 species or an accurate functional analysis. [13]

141 Whole metagenome sequencing(WMS) allows us to achieve a satisfactory
142 resolution of the microbiome. Earlier we have used the WMS data to characterize the
143 gut microbiota in NAFLD patients with and without advanced fibrosis and identified
144 37 differential bacterial species, among which the abundance of *Escherichia coli* and
145 *Bacteroides vulgatus* was increased in patients with advanced fibrosis and it's
146 association with microbial metabolites.[9, 14-16] WMS data were also used to study
147 the interactions between the gut microbiome and steatosis in obesity.[15, 17]
148 However, a similar study is lacking for the comparison of the gut community between
149 healthy and NAFLD subjects using WMS data, which is our goal in this study. Here
150 we report the structural and functional characteristics of the gut microbiome in
151 NAFLD, and its association with BA metabolism.

152

153 **Results**

154 *Gut microbiota alterations between NAFLD patients and healthy controls*

155 WMS data from 86 well-characterized biopsy-proven NAFLD patients and 38 healthy
156 controls with similar characteristics (Table 1 and Table S1) were chosen to study the

157 structural and functional differences in gut microbiota between NAFLD patients and
158 healthy controls. And we have confirmed that gender or age distribution did not
159 account for the observed microbial differences in this study (Figure S1).

160 *Compositional changes in NAFLD gut microbiota*

161 We determined the microbial compositions of NAFLD and healthy controls using
162 WMS data. Bacteroidetes, Firmicutes, Actinobacteria and Proteobacteria were the
163 dominant phyla that collectively account for around 90% proportions in both groups
164 (Figure S2A). NAFLD individuals had lower bacterial diversity than healthy controls
165 (Figure S2B). Besides, significant compositional differences were observed between
166 these two groups (Figure S2C).

167 To identify microbial markers that may distinguish NAFLD from healthy subjects,
168 differential species were determined with Mann-Whitney U-tests. 53 species with
169 FDR values < 0.1 were identified as differential species (Figure 1 & Table S2).

170 Among these, 11 species were dominant in NAFLD patients, which mainly belong to
171 Clostridia class, including *Eubacterium siraeum*, *Clostridium bolteae*, *E. coli* and
172 *B.ovatus*, *B.stercoris* from Bacteroidia class. On the other hand, 42 species
173 significantly reduced in NAFLD patients were mainly of Bacteroidia class, including,
174 *Bacteroides dorei*, *Alistipes shahii*, and of Clostridia class, for instance, *Eubacterium*
175 *eligens*, *Eubacterium hallii*, and *Faecalibacterium prausnitzii*. In addition, random
176 forest (RF) model constructed with differential species achieved an AUC of 0.97 to
177 detect NAFLD patients from controls (Figure S3).

178 *Ecological structural changes in NAFLD gut microbiota*

179 Furthermore, at whole-community level, microbial interaction analysis was performed
180 to investigate potential changes in ecological structure. There were more species in
181 healthy communities than those in NAFLD communities (167 nodes vs 141 nodes)
182 though with similar amount of interactions. Then, we examined the “core community”
183 (interactions with magnitudes > 0.4) of healthy and NAFLD groups, respectively.
184 Considerable discrepancies existed in the “core community” of healthy and NAFLD
185 (Figure 2A&B). In detail, the healthy “core community” was more complex, with 162
186 species and 565 interactions, compared to the NAFLD community with 81 species
187 and 166 interactions. And the NAFLD community was separated into 8 isolated
188 components, an indication of unstable microbial community. Among them, the major
189 component harbored most species from Clostridia class, such as BA production
190 bacteria, *C.bolteae* (node NO. 78), *C.clostridioforme* (node NO. 138) with increased
191 proportion in NAFLD, while species from Bacilli class were dominant in the second
192 major component. Besides, species with increased abundance in NAFLD patients
193 (circle nodes in Figure 2B) were dominant in the “core community” and positively
194 interacted with each other. Then, we looked into the top 20 hub species of “core
195 community”, respectively. 10 of them were common in both group, such as *C.bolteae*,
196 *C.hathewayi*, *Dorea longicatena*, *Flavonifractor plautii*, which may play the role as
197 the “keystone” to sustain the homeostasis (Figure 2C&D).

198

199 *Functional changes in NAFLD gut microbiota*

200 Microbial functional profiles were determined at pathway level using HUMAnN2 and
201 92 differential pathways were identified between the NAFLD and the healthy groups
202 (Table S3). Similarly, we identified 8 important pathway features (Figure 3A) to build
203 RF model (AUC=0.83) that could distinguish NAFLD patients from healthy subjects
204 (Figure 3B). Most pathways were more represented in NAFLD microbiota than in
205 controls. These pathways included secondary BA synthesis (ko00121) (Figure 3C),
206 benzoate degradation (ko00362), biosynthesis of ansamycins (ko01051) and oxidative
207 phosphorylation (ko00190) (Figure S4).

208 *Novel genes and microbial genomes associated with secondary BA synthesis*

209 The fact that the secondary BAs biosynthesis pathway was significantly elevated in
210 NAFLD (Figure 3C) prompted us to examine the relevant BA metabolizing enzymes
211 encoded by the microbiome. Taking advantage of the WMS data, we were able to
212 quantify the gene abundance and to map these genes to specific microbial genomes.

213 *Genes related to secondary BA synthesis*

214 Bacterial genes directly involved in secondary BA synthesis catalyze the
215 deconjugation, the oxidation and epimerization, or the multi-step 7 α -dehydroxylation
216 reactions (Figure 4A). Protein sequences of target enzymes were collected from
217 Integrated Microbial Genomes(IMG) database (Figure 4A).[18] High quality protein
218 sequences were selected to construct hidden Markov models(HMMs), in order to

219 identify potential BA metabolizing enzymes.

220 The data (Figure 4B) showed that genes encoding 7-alpha-hydroxysteroid
221 dehydrogenase(7 α -HSDH), BSH and bile acid inducible operon (bai)A, baiB, baiCD,
222 baiH were relatively more abundant than baiE, baiF and baiI. Importantly,
223 significantly increased abundance of 7 α -HSDH, baiA and baiB were observed in
224 NAFLD compared to controls. These data were consistent with the pathway analysis
225 results, and confirmed the increased secondary BA production in NAFLD.[12]

226 *Novel identification of microbial genomes related to secondary BA synthesis*
227 *using advanced bioinformatics*

228 To identify the BA metabolizing microbial genomes, the metagenomic-assembled
229 species(MAG) analysis was performed. Prevalent genes in the non-redundant gene
230 catalog that presented in more than 5 samples were binned into 252 MAGs, which
231 were considered to represent distinct microbial genomes. Among these, 50 MAGs that
232 contain at least one gene encoding BSH, HSDH or bile acid inducible operons (Table
233 S4) were defined as BA-metabolizing MAG. To obtain relatively complete microbial
234 genomes, we re-assembled these 50 MAGs using high quality reads mapped to genes
235 in each MAG.

236 Among these, 10 MAGs exhibited significantly increased abundance in NAFLD,
237 while 18 MAGs were reduced in NAFLD (Figure 5A). Among the 10 MAGs elevated
238 in NAFLD, 6 MAGs belong to Bacteroides (order Bacteroidales), including

239 *B.vulgatus*, *B.ovatus*, and *B.stercoris*. Other MAG genomes were assigned as
240 *E.rectale* and *E.biforme* (order Clostridiales). BA-metabolizing MAGs with reduced
241 abundance in NAFLD are mainly from *R.bromii*, *D.longicatena* and *B. dorei*.
242 Furthermore, we explored the species' contributions of pathways in via HUMAnN2,
243 and found that the pathway secondary bile acids biosynthesis were mainly encoded by
244 *E.eligens* (48.3%) and *B.vulgatus* (26.2%)(Figure S5). This is consistent with the
245 increased BA-metablizing MAGs belonging to species *Bacteroides vulgatus* and
246 *Eubacterium eligens*.

247 For a better understanding of the BA metabolizing microbial community, microbial
248 interactions analysis was performed with BA-metabolizing MAGs. In contrast to the
249 situation where more interactions existed in healthy group on whole-community level,
250 we found that the sub-network of BA-metabolizing MAG was more complex with
251 considerable interactions in NAFLD than in controls (164 and 100 edges,
252 respectively) (Figure 5B &C). In addition, most MAGs with higher proportions in
253 NAFLD patients were hub nodes in both healthy and NAFLD BA-metabolizing
254 communities and were positively interacted, such as *Bacteroides sp.* MAG001,
255 *B.vulgatus* MAG007, *B.ovatus* MAG026, *B.vulgatus* MAG030 and *B.xylanisolvens*
256 MAG117. These are likely "house-keeping" species for BA metabolism. In contrast,
257 *Bacteroides stercoris* MAG003, an MAG not included in the healthy network, was
258 highly elevated in NAFLD, ranked high in the NAFLD network, and positively
259 interacted with the "house-keeping" BA metabolizing species. Similarly, *E.biforme*

260 MAG036 and MAG089, which exhibited the lowest hub score in healthy network,
261 ranked the highest in NAFLD network.

262 In general, the observed species were represented by multiple MAGs. Here,
263 *R.bromii* was represented by 7 MAGs, and *E.eligens* by 5 MAGs. However, only one
264 of the 7 *R.bromii* MAG was significantly increased in NAFLD group, while 4 others
265 showed decreased abundance (Table S5). Situations were similar in *B.vulgatus* (two
266 of three increased) and *E.rectale* (one increased and two decreased). Unexpectedly,
267 multiple MAGs of the same species were distributed in different modules both in
268 healthy and NAFLD communities (Table S6). Apparently, these observations indicate
269 that strains within the same species may function differently.

270 ***Different BA metabolizing potentials among NAFLD microbiota and***
271 ***emergence of two subtypes of NAFLD: High BA versus normal BA subtype***

272 Although the average abundances of the secondary BA metabolism pathway and
273 related genes were increased in NAFLD, we noticed that the abundances exhibited a
274 broad distribution among NAFLD patients (Figure 3C and 4B). Many of the NAFLD
275 microbiota exhibited BA metabolizing potentials similar to those of healthy controls.
276 Based on the abundance of 3 differential BA-metabolizing genes (*7 α -HSDH*, *baiA*
277 and *baiB*), NAFLD patients were clustered into two subtypes: normal-BA subtype
278 comprising 45 patients and high-BA subtype comprising 37 patients (Figure 6A),
279 which was not related to the disease severity ($p=0.7$). The abundances of the 3 marker
280 genes were all significantly higher in high-BA subtype, but were similarly represented

281 between normal-BA subtype and healthy control group (Figure 6B). In addition, we
282 performed the PCA analysis based on the entire differential microbial enzymes and
283 found that the normal-BA subtype and the healthy control group exhibited closer
284 distance, as compared to the high-BA group (Figure 6C). In further characterization of
285 the microbial profiles of the patterns of the normal-BA and high-BA groups, we
286 identified 3 species (Table S7), 68 enzymes (Table S8) and 16 pathways (Table S9)
287 that could distinguish the normal-BA subtype from the high-BA subtype, and, at the
288 same time, could distinguish NAFLD from the healthy group. Based on the relative
289 abundance of these differential features, the study subjects were clustered into three
290 groups consistent with their BA metabolizing potentials. Features were also clustered
291 into two groups (Figure S6). One group (including species *Flavonifractor plautii*,
292 enzymes 2-dehydropantoate 2-reductase and glutamate 5-kinase and pathway
293 glycosaminoglycan degradation etc.) exhibited elevated abundance in normal-BA
294 subtype and reduced abundance in high-BA subtype. The other group (including
295 species *Escherichia coli* and *Ruminococcus bromii*, enzymes glycerol dehydrogenase,
296 agmatinase and pathway citrate cycle, phosphotransferase system etc.) exhibited an
297 opposite distribution among the study groups.

298 ***Elevated secondary BA synthesis capability in the validation cohort of***
299 ***NAFLD***

300 Similar analyses were performed with the validation dataset. The secondary BA
301 synthesis genes 7α -HSDH, BSH, baiA, baiB, baiCD, baiF, and baiH were relatively

302 more abundant than baiE and baiI. Importantly, significantly increased abundance of
303 most secondary BA synthesis genes were observed in NAFLD compared to controls
304 (Figure S7).

305 As for BA metabolizing microbial genomes, we identified 13 MAGs, each carrying
306 at least one gene encoding BSH, HSDH or bai operon. Among these, 9 MAGs
307 exhibited a trend of increased abundance in NAFLD. Consistent with the discovery
308 cohort, these 9 MAGs belonged to *B. vulgatus*, and *R. bromii*(Table S10). Statistical
309 significance was not achieved for the increased abundances of the MAGs, likely due
310 to the small sample size.

311 **Discussion**

312 In this study, we defined the structural and functional differences in gut microbiota
313 between NAFLD and healthy subjects, at the resolutions of gene, species and strain.
314 The current study is novel in using WGS data to compare the gut microbiota between
315 NAFLD and healthy controls and underpinning the role of BA metabolizing
316 microbiome in NAFLD, and potentially identifying two microbiota-derived subtypes
317 of NAFLD that may have clinical implications for both biomarker as well as
318 therapeutic development. Compared with the approach of 16S rRNA sequencing,
319 WMS data allow direct function quantification and accurate taxa assignment of the
320 entire gut microbiome, at the levels of species and strain. Out of the many differential
321 representations of genes and species between NAFLD and healthy controls, one
322 outstanding observation is the increased abundance of secondary BA metabolizing

323 genes and microbes in NAFLD and that BA metabolizing bacteria were dominant taxa
324 in the gut of NAFLD. For the first time, we identified the genes and bacterial strains
325 responsible for elevated secondary BA synthesis in NAFLD. Similarly, increased
326 abundances of the BA metabolizing genes and bacterial species were observed in an
327 independent validation cohort. Considering the profound impact of BA signaling on
328 lipid and carbohydrate metabolism[19], the differential BA metabolizing genes and
329 bacterial strains we identified may serve as novel therapeutic targets for NAFLD
330 management.

331 We and others have reported elevated secondary BA production in NAFLD. [12,
332 20] In our previous study[12], we observed much increased secondary BAs in
333 NAFLD serum and consistently, an elevated taurine metabolizing microbiota, an
334 indication of increased BA metabolism in the gut. However, we did not observe any
335 significant change in the abundance of those microbes that directly metabolize BA
336 (that is, microbes encoding BSH, 7-alpha-HSDH and 7-alpha-dehydroxylase), likely
337 because the 16S rRNA sequencing approach was not able to provide a sufficient
338 resolution for functional analysis. With the advantage WGS data, the current study
339 was able to provide convincing evidence at a satisfactory resolution, that secondary
340 BA synthesis enzymes and microbes with secondary BA metabolizing potentials were
341 indeed elevated in NAFLD gut microbiota. As secondary BAs are potent antagonistic
342 ligands for FXR, data presented here is a strong support for the hypothesis that

343 elevated secondary BA synthesis by the microbiota contributes to NAFLD

344 etiology.[12, 21]

345 Although on average NAFLD patients exhibited elevated BA metabolizing

346 microbiota, and higher serum DCA (secondary BA) when compared to healthy

347 controls, our data showed that elevated BA metabolizing microbiota was not a

348 unanimous phenomenon in NAFLD. More than half of the NAFLD patients (45 out of

349 82) had a microbiota with normal BA metabolizing potential. Based on BA

350 metabolizing potentials, our NAFLD patients can be clustered into two subtypes. This

351 indicates that BA related pathomechanism does not apply to many NAFLD patients,

352 in line with the current multi-hit hypothesis.[3] Besides the difference in BA

353 metabolizing potentials, these two subtypes of the gut microbiota also exhibit

354 different abundances in other genes, pathways, and bacterial species. It is interesting

355 to note that NAFLD microbiota with higher BA metabolizing potentials also exhibited

356 elevated representation of *E.coli*, a potent alcohol producer[6, 22], suggesting that the

357 gut microbiota may impact NAFLD pathogenesis through multiple mechanisms in the

358 same patient.

359 BA based therapies such as obeticholic acid has been shown to improve NASH.

360 [23] However, the response rates to OCA in improvement of one-stage of fibrosis in

361 the FLINT trial was 35% versus 19% in placebo.[24] It is plausible that NAFLD

362 patients with altered BA subtype may be more likely to respond to BA based therapies

363 and those with a normal BA subtype should receive an alternate strategy paving the
364 pay for a microbiome based precision medicine tool in NASH therapeutics.

365 Another outstanding observation in this study is that many strains of the same
366 species are functionally different. Specifically, different strains of *Bacteroides ovatus*
367 were clustered into different functional modules (modules 0, 2, 4 in healthy
368 communities and modules 3, 4, 6 in NAFLD communities). It is also interesting to
369 note that only one of the four observed strains of *Bacteroides ovatus* was significantly
370 increased in NAFLD group. Similar observations were reported for *F. prausnitzii*[25,
371 26] and *E.coli*[27, 28], suggesting the genomic variability within a microbial
372 species.[29] Some of the microbiome studies based on 16S rRNA platforms may need
373 a re-evaluation because of this genomic variability.

374 It was interesting to note that 10 BA-metabolizing bacterial strains, including
375 *B.stercoris*, *E.biforme*, and *R.bromii*, were elevated and were dominant strains in
376 NAFLD microbiota. These BA-metabolizing strains belong to two different phylum.
377 Zhao et al. proposed a concept in gut microbiota that a group of species that “exploit
378 the same class of environmental resources in a similar way” may be considered as a
379 “guild” in ecology[30] and members of a guild do not necessarily share taxonomic
380 similarity, but they co-occur when adapting to the changing environment.[25]
381 Similarly, the 10 BA-metabolizing strains may act as a synergetic guild to promote
382 the secondary BA production in the NAFLD microbial community. There were more
383 positive interactions among these 10 strains in NAFLD community than in healthy

384 community, indicating elevated capabilities of secondary BA production and
385 intensified competition among these secondary BA producers within the microbial
386 guild of NAFLD. It is likely that these strains are responsible for elevated secondary
387 BA production in NAFLD, contributing to NAFLD pathogenesis.[12] Among these
388 10 strains, MAG036 , MAG089 , and MAG003 with increased abundance and the
389 highest network importance in NAFLD may act as the “keystone” species[53], and
390 therefore, represent potential targets for intervention.

391 At the whole community level, the NAFLD gut microbiota exhibited significantly
392 reduced diversity compared to the healthy controls. In addition, much reduced
393 interactions among the members of the NAFLD gut microbiota were observed. With
394 less strains and sparse interactions, the gut microbial community in NAFLD is
395 relatively weak and unstable. Similarly, reduced biodiversity were reported in the gut
396 of obesity.[31] It is postulated that long-term dietary habit is the major cause for the
397 altered gut microbiota.[32] The biodiversity disaster in the gut of humans demands
398 immediate attention. The restoration of the gut microbial diversity may, at the same
399 time, prevent or cure many of the microbiota related diseases including NAFLD.

400 In summary, we identified specific genes and bacterial strains responsible for
401 elevated secondary BA production in NAFLD. These genes and strains may serve as
402 novel therapeutic targets for microbiome-based high-BA subtype of NAFLD. These
403 findings strongly support our hypothesis that elevated secondary BA synthesis
404 contributes to the development of NAFLD. In addition, our WGS study revealed the

405 heterogeneity of the gut microbiota among NAFLD patients highlighting the
406 importance of personalized treatment for NAFLD. Our study also revealed many
407 other microbial characteristics of the NAFLD that demands attention such as the
408 much reduced diversity and the ecological guild in the gut of NAFLD.

409 **Materials and Methods**

410 *Data information and preprocessing*

411 Discovery dataset: The NAFLD datasets and relevant meta data(Sequence Read
412 Archive, PRJNA373901) were described previously[9] comprising 86 biopsy-proven
413 NAFLD patients. The healthy control dataset was from PRJEB6070[33], with 38
414 healthy individuals with BMI < 25. These subjects were chosen because of similar
415 age and gender ratio compared to NAFLD patients to effectively reduce bias[34]
416 (Table 1 & Table S1).

417 Validation dataset: 10 middle-aged NAFLD subjects [35] (PRJNA420817) were
418 recruited to a diet trial and the initial baseline data before diet intervention were used
419 for this study. 11 healthy subjects from MetaHit Project[36](Sequence Read Archive,
420 PRJEB1220) with similar age and gender ratio were chosen as controls (Table 1 &
421 Table S1).

422 All subjects provided a written informed consent and the study protocol was
423 approved by Institutional Review Board (approval number:UCSD IRB11298) or
424 registered at ClinicalTrials.gov with identifier: NCT02558530.

425 The KneadData(<http://huttenhower.sph.harvard.edu/kneaddata>) tool was used to
426 ensure the data consisted of high quality microbial reads free from contaminants. The
427 low quality reads were removed using Trimmomatic(SLIDINGWINDOW:4:15
428 MINLEN:75 LEADING:10 TRAILING:10). The remaining reads were mapped to the
429 human genome(hg38) by bowtie2[37], and the matching reads were removed as
430 contaminant reads from the host.

431 ***Gene-based taxonomic and functional profiling of gut microbiota***

432 MetaPhlAn2[38] was used to identify the composition of gut microbial community
433 and to assess the abundance of the prokaryotes within each sample. Species that failed
434 to exceed 0.01% relative abundance in at least 20% samples were excluded.

435 The functional profiling of gut microbiome was determined by the HMP Unifiled
436 Metabolic Analysis Network (HUMAN2)[39]. In brief, high-quality metagenomic
437 reads were mapped to the pangenomes of species identified with MetaPhlAn2 and
438 these pangenomes have been pre-annotated by UniRef90 families. Reads failed to
439 map to a pangenome were aligned to UniRef90 by translated search with
440 DIAMOND[40]. Hits to UniRef90 are weighted according to alignment quality,
441 sequence length and coverage. In this study, enzyme abundance was quantified by
442 regrouping (summed) according to EC number and pathway abundance by regrouping
443 (summed) genes in pathways against KEGG database.

444 ***Identification of genes required for secondary BA synthesis***

445 To identify genes that encode enzymes catalyzing secondary BA synthesis, hidden
446 Markov models (HMMs) of BA-related genes were constructed. Secondary BA
447 synthesis mainly involves (1) deconjugation, (2) oxidation and epimerization and (3)
448 multi-step 7 α -dehydroxylation. Enzymes participating in these processes are bile salt
449 hydrolase (BSH), hydroxysteroid dehydrogenase (HSDH) and enzymes required in
450 the multi-step 7 α -dehydroxylation (including baiA, baiB, baiCD, baiE, baiF, baiH and
451 baiI).[18] Representative protein sequences of target enzymes were obtained from
452 Integrated Microbial Genomes (IMG) database[41]. High quality sequences were
453 selected and aligned in Clustal Omega[42] before they were used to construct HMMs
454 on full-length proteins via hmmbuild in HMMER(3.1b2)[43]. Model seed sequences
455 were realigned to the model using hmalign (default mode) before rebuilding models
456 based on the obtained alignments until both model length and relative entropy per
457 position were constant. Subsequently, all protein sequences in non-redundant gene
458 catalog were screened (hmmsearch) for candidate protein sequences and sequences
459 with hmmscore > lower quartile score and e-value less than 10⁻⁵ were identified as
460 potential secondary BA synthesis associated genes.

461 ***Assembly-based microbial genomes***

462 For functional analysis of the microbial genomes, we performed bin-based microbial
463 genome assembly with the WMS data, including de novo assembly and non-redundant

464 human gut gene catalog construction, co-abundance clustering and determination of
465 metagenome-assembled genomes (MAG), MAG-augmented assembly and taxonomic
466 annotation.

467 *De novo assembly and non-redundant human gut gene catalog construction*

468 High-quality paired-end reads from each sample were used for de novo assembly with
469 Megahit[44] into contigs of at least 500-bp length. Genes were predicted on the
470 contigs with MetaGeneMark[45]. A non-redundant gene catalog related to NAFLD
471 was constructed with CD-HIT[46] using a sequence identity cut-off of 0.95, with a
472 minimum coverage cut-off of 0.9 for the shorter sequences and 11,348,567 microbial
473 genes were contained.

474 *Co-abundance clustering and determination of MAG*

475 Bowtie2 was used to align high quality reads to the non-redundant gene catalog.
476 Aligned results were random sampled and downsized to 15 million per sample
477 (FR-173, FR-719, FR-730, SRR4275396, SRR4275459, SRR4275469, SRR4275470
478 were excluded for not enough reads) to adjust for sequencing depth and technical
479 variability. The soap.coverage script (available at:
480 <http://soap.genomics.org.cn/down/soap.coverage.tar.gz>) was used to calculate
481 gene-length normalized base counts and the gene abundance profiling was calculated
482 as the average abundance of 30 times of repeated sampling. All the genes were
483 clustered into MAG using MSPminer[47] based on their abundance with default

484 parameters.

485 *MAG-augmented assembly and taxonomic annotation*

486 We performed augmented assembly for target MAG. Briefly, the MAG- and
487 sample-specific reads were derived by aligning all high-quality reads to the MAG
488 gene contigs with Burrows-Wheeler Aligner (0.7.17)[48], followed by de novo
489 assembly with SPAdes(3.13.0)[49] using k-mers from 21 to 55. CVtree3.0 web
490 server[50] was used to identify the taxonomy of the MAGs, which applies a
491 composition vector to perform phylogenetic analysis.

492 *Statistic analysis*

493 *Differential features identification*

494 Compositional features and functional features that present in at least 20% of the
495 samples and with average relative abundance over 0.01% in each group were selected
496 for further differential analysis. Differential features were identified by two-tailed
497 Mann-Whitney U-tests adjusted by Benjamini-Hochberg. Features with an FDR value
498 < 0.05 (FDR values < 0.1 for species) were identified as differential features. Then
499 differential compositional and functional feature profiles were used to build random
500 forest(RF) model using RandomForest package in R. Feature importance were
501 estimated via gini importance and then the best model were rebuilt by adding features
502 according to their importance ranks. Area Under the Receiver-Operator Curve(AUC)
503 was used to measure the accuracy of the models.

504 *Microbial interaction analysis*

505 SparCC[51] was performed to construct compositionality-corrected microbial
506 interactions network, which is capable of estimating correlation values from
507 compositional data. Interactions were calculated with 100 refining interactions, after
508 which statistical significance of each interaction was estimated with 1000
509 permutations. Only interactions with p value < 0.05 were included in downstream
510 analysis and those interactions with magnitudes > 0.4 were included in the “core
511 community”. The importance of species in the community was calculated using
512 Hyperlink-Induced Topic Search(HITS) algorithms in Python package ‘networkx’.
513 The networks were then visualized with Cytoscape[52] and module analysis was
514 performed with ModuLand in Cytoscape.

515 *Other statistics*

516 Analysis of similarities (ANOSIM) was performed based on distance matrix for
517 statistical comparisons of samples between groups or subtypes. P value was calculated
518 using 9999 permutations. $p < 0.05$ indicates significant difference. Heatmap was
519 plotted via “pheatmap” package in R, and features were clustered based on euclidean
520 distance by “ward.D”. Differential features among healthy, normal-BA and high-BA
521 groups were identified with Dunn tests adjusted by Benjamini–Hochberg, and features
522 with FDR values < 0.05 were determined as significant differential features.

523 **References**

- 524 [1] Younossi Z, Anstee QM, Marietti M, Hardy T, Henry L, Eslam M, George J,
525 Bugianesi E. Global burden of NAFLD and NASH: trends, predictions, risk
526 factors and prevention. *Nat Rev Gastroenterol Hepatol* 2018;15(1):11-20.
- 527 [2] Arab JP, Arrese M, Trauner M. Recent Insights into the Pathogenesis of
528 Nonalcoholic Fatty Liver Disease. *Annu Rev Pathol-Mech* 2018;13:321-50.
- 529 [3] Tilg H, Moschen AR. Evolution of Inflammation in Nonalcoholic Fatty Liver
530 Disease: The Multiple Parallel Hits Hypothesis. *Hepatology*
531 2010;52(5):1836-46.
- 532 [4] Piguet AC, Guarino M, Potaczek DP, Garn H, Dufour JF. Hepatic gene
533 expression in mouse models of NAFLD after acute exercise. *Hepatol Res*
534 2019;49(6):637-52.
- 535 [5] Margini C, Dufour JF. The story of HCC in NAFLD: from epidemiology,
536 across pathogenesis, to prevention and treatment. *Liver Int* 2016;36(3):317-24.
- 537 [6] Zhu L, Baker SS, Gill C, Liu WS, Alkhouri R, Baker RD, Gill SR.
538 Characterization of Gut Microbiomes in Nonalcoholic Steatohepatitis (NASH)
539 Patients: A Connection Between Endogenous Alcohol and NASH. *Hepatology*
540 2013;57(2):601-9.
- 541 [7] Michail S, Lin M, Frey MR, Fanter R, Paliy O, Hilbush B, Reo NV. Altered
542 gut microbial energy and metabolism in children with non-alcoholic fatty liver
543 disease. *FEMS Microbiol Ecol* 2015;91(2):1-9.
- 544 [8] Boursier J, Mueller O, Barret M, Machado M, Fizanne L, Araujo-Perez F, Guy
545 CD, Seed PC, Rawls JF, David LA, Hunault G, Oberti F, Cales P, Diehl AM.
546 The severity of nonalcoholic fatty liver disease is associated with gut dysbiosis
547 and shift in the metabolic function of the gut microbiota. *Hepatology*
548 2016;63(3):764-75.
- 549 [9] Loomba R, Seguritan V, Li W, Long T, Klitgord N, Bhatt A, Dulai PS, Caussy
550 C, Bettencourt R, Highlander SK, Jones MB, Sirlin CB, Schnabl B, Brinkac L,
551 Schork N, Chen CH, Brenner DA, Biggs W, Yooseph S, Venter JC, Nelson
552 KE. Gut Microbiome-Based Metagenomic Signature for Non-invasive
553 Detection of Advanced Fibrosis in Human Nonalcoholic Fatty Liver Disease.
554 *Cell Metab* 2017;25(5):1054-62 e5.
- 555 [10] Mouzaki M, Wang AY, Bandsma R, Comelli EM, Arendt BM, Zhang L, Fung
556 S, Fischer SE, McGilvray IG, Allard JP. Bile Acids and Dysbiosis in
557 Non-Alcoholic Fatty Liver Disease. *PLoS One* 2016;11(5):e0151829.
- 558 [11] Zhu L, Baker RD, Zhu R, Baker SS. Y Sequencing the Gut Metagenome as a
559 Noninvasive Diagnosis for Advanced Nonalcoholic Steatohepatitis.
560 *Hepatology* 2017;66(6):2080-3.
- 561 [12] Jiao N, Baker SS, Nugent CA, Tsompana M, Cai L, Wang Y, Buck MJ, Genco
562 RJ, Baker RD, Zhu R, Zhu L. Gut microbiome may contribute to insulin

- 563 resistance and systemic inflammation in obese rodents: a meta-analysis.
564 *Physiological Genomics* 2018;50(4):244-54.
- 565 [13] Sharpton SR, Ajmera V, Loomba R. Emerging Role of the Gut Microbiome in
566 Nonalcoholic Fatty Liver Disease: From Composition to Function. *Clin*
567 *Gastroenterol Hepatol* 2018;17(2):296-306.
- 568 [14] Caussy C, Hsu C, Lo MT, Liu A, Bettencourt R, Ajmera VH, Bassirian S,
569 Hooker J, Sy E, Richards L, Schork N, Schnabl B, Brenner DA, Sirlin CB,
570 Chen CH, Loomba R, Genetics of NiTC. Link between gut-microbiome
571 derived metabolite and shared gene-effects with hepatic steatosis and fibrosis
572 in NAFLD. *Hepatology* 2018;68(3):918-32.
- 573 [15] Caussy C, Loomba R. Gut microbiome, microbial metabolites and the
574 development of NAFLD. *Nat Rev Gastroenterol Hepatol* 2018;15(12):719-20.
- 575 [16] Caussy C, Hsu C, Singh S, Bassirian S, Kolar J, Faulkner C, Sinha N,
576 Bettencourt R, Gara N, Valasek MA, Schnabl B, Richards L, Brenner DA,
577 Hofmann AF, Loomba R. Serum bile acid patterns are associated with the
578 presence of NAFLD in twins, and dose-dependent changes with increase in
579 fibrosis stage in patients with biopsy-proven NAFLD. *Aliment Pharmacol*
580 *Ther* 2019;49(2):183-93.
- 581 [17] Hoyles L, Fernandez-Real JM, Federici M, Serino M, Abbott J, Charpentier J,
582 Heymes C, Luque JL, Anthony E, Barton RH, Chilloux J, Myridakis A,
583 Martinez-Gili L, Moreno-Navarrete JM, Benhamed F, Azalbert V,
584 Blasco-Baque V, Puig J, Xifra G, Ricart W, Tomlinson C, Woodbridge M,
585 Cardellini M, Davato F, Cardolini I, Porzio O, Gentileschi P, Lopez F,
586 Foufelle F, Butcher SA, Holmes E, Nicholson JK, Postic C, Burcelin R,
587 Dumas ME. Molecular phenomics and metagenomics of hepatic steatosis in
588 non-diabetic obese women. *Nat Med* 2018;24(7):1070-80.
- 589 [18] Ridlon JM, Harris SC, Bhowmik S, Kang DJ, Hylemon PB. Consequences of
590 bile salt biotransformations by intestinal bacteria. *Gut Microbes*
591 2016;7(1):22-39.
- 592 [19] Arab JP, Karpen SJ, Dawson PA, Arrese M, Trauner M. Bile acids and
593 nonalcoholic fatty liver disease: Molecular insights and therapeutic
594 perspectives. *Hepatology* 2017;65(1):350-62.
- 595 [20] Ferslew BC, Xie G, Johnston CK, Su M, Stewart PW, Jia W, Brouwer KL,
596 Barritt AS. Altered Bile Acid Metabolome in Patients with Nonalcoholic
597 Steatohepatitis. *Dig Dis Sci* 2015;60(11):3318-28.
- 598 [21] Jiao N, Baker SS, Chapa-Rodriguez A, Liu W, Nugent CA, Tsompana M,
599 Mastrandrea L, Buck MJ, Baker RD, Genco RJ, Zhu R, Zhu L. Suppressed
600 hepatic bile acid signalling despite elevated production of primary and
601 secondary bile acids in NAFLD. *Gut* 2018;67(10):1881-91.
- 602 [22] Clark DP. The fermentation pathways of *Escherichia coli*. *FEMS Microbiol*
603 *Rev* 1989;5(3):223-34.

- 604 [23] Perazzo H, Dufour JF. The therapeutic landscape of non-alcoholic
605 steatohepatitis. *Liver Int* 2017;37(5):634-47.
- 606 [24] Neuschwander-Tetri BA, Loomba R, Sanyal AJ, Lavine JE, Van Natta ML,
607 Abdelmalek MF, Chalasani N, Dasarathy S, Diehl AM, Hameed B, Kowdley
608 KV, McCullough A, Terrault N, Clark JM, Tonascia J, Brunt EM, Kleiner DE,
609 Doo E, Network NCR. Farnesoid X nuclear receptor ligand obeticholic acid
610 for non-cirrhotic, non-alcoholic steatohepatitis (FLINT): a multicentre,
611 randomised, placebo-controlled trial. *Lancet* 2015;385(9972):956-65.
- 612 [25] Zhao L, Zhang F, Ding X, Wu G, Lam YY, Wang X, Fu H, Xue X, Lu C, Ma
613 J, Yu L, Xu C, Ren Z, Xu Y, Xu S, Shen H, Zhu X, Shi Y, Shen Q, Dong W,
614 Liu R, Ling Y, Zeng Y, Wang X, Zhang Q, Wang J, Wang L, Wu Y, Zeng B,
615 Wei H, Zhang M, Peng Y, Zhang C. Gut bacteria selectively promoted by
616 dietary fibers alleviate type 2 diabetes. *Science* 2018;359(6380):1151-6.
- 617 [26] Zhang C, Yin A, Li H, Wang R, Wu G, Shen J, Zhang M, Wang L, Hou Y,
618 Ouyang H, Zhang Y, Zheng Y, Wang J, Lv X, Wang Y, Zhang F, Zeng B, Li
619 W, Yan F, Zhao Y, Pang X, Zhang X, Fu H, Chen F, Zhao N, Hamaker BR,
620 Bridgewater LC, Weinkove D, Clement K, Dore J, Holmes E, Xiao H, Zhao G,
621 Yang S, Bork P, Nicholson JK, Wei H, Tang H, Zhang X, Zhao L. Dietary
622 Modulation of Gut Microbiota Contributes to Alleviation of Both Genetic and
623 Simple Obesity in Children. *EBioMedicine* 2015;2(8):968-84.
- 624 [27] Kaas RS, Friis C, Ussery DW, Aarestrup FM. Estimating variation within the
625 genes and inferring the phylogeny of 186 sequenced diverse *Escherichia coli*
626 genomes. *Bmc Genomics* 2012;13.
- 627 [28] Salipante SJ, Roach DJ, Kitzman JO, Snyder MW, Stackhouse B, Butler-Wu
628 SM, Lee C, Cookson BT, Shendure J. Large-scale genomic sequencing of
629 extraintestinal pathogenic *Escherichia coli* strains. *Genome Research*
630 2015;25(1):119-28.
- 631 [29] Mallick H, Ma SY, Franzosa EA, Vatanen T, Morgan XC, Huttenhower C.
632 Experimental design and quantitative analysis of microbial community
633 multiomics. *Genome Biol* 2017;18(1):228.
- 634 [30] Simberloff D, Dayan T. The Guild Concept and the Structure of Ecological
635 Communities. *Annu Rev Ecol Syst* 1991;22:115-43.
- 636 [31] Menni C, Jackson MA, Pallister T, Steves CJ, Spector TD, Valdes AM. Gut
637 microbiome diversity and high-fibre intake are related to lower long-term
638 weight gain. *Int J Obes (Lond)* 2017;41(7):1099-105.
- 639 [32] Xu Z, Knight R. Dietary effects on human gut microbiome diversity. *Br J Nutr*
640 2015;113 Suppl:S1-5.
- 641 [33] Zeller G, Tap J, Voigt AY, Sunagawa S, Kultima JR, Costea PI, Amiot A,
642 Bohm J, Brunetti F, Habermann N, Hercog R, Koch M, Luciani A, Mende DR,
643 Schneider MA, Schrotz-King P, Tournigand C, Tran Van Nhieu J, Yamada T,
644 Zimmermann J, Benes V, Kloor M, Ulrich CM, von Knebel Doeberitz M,

- 645 Sobhani I, Bork P. Potential of fecal microbiota for early-stage detection of
646 colorectal cancer. *Mol Syst Biol* 2014;10:766.
- 647 [34] Cochran WG, Rubin DB. Controlling Bias in Observational Studies: A
648 Review. *Matched Sampling for Causal Effects* 2006:30-57.
- 649 [35] Mardinoglu A, Wu H, Bjornson E, Zhang C, Hakkarainen A, Rasanen SM,
650 Lee S, Mancina RM, Bergentall M, Pietilainen KH, Soderlund S, Matikainen
651 N, Stahlman M, Bergh PO, Adiels M, Piening BD, Graner M, Lundbom N,
652 Williams KJ, Romeo S, Nielsen J, Snyder M, Uhlen M, Bergstrom G, Perkins
653 R, Marschall HU, Backhed F, Taskinen MR, Boren J. An Integrated
654 Understanding of the Rapid Metabolic Benefits of a Carbohydrate-Restricted
655 Diet on Hepatic Steatosis in Humans. *Cell Metab* 2018;27(3):559-71 e5.
- 656 [36] Qin J, Li R, Raes J, Arumugam M, Burgdorf KS, Manichanh C, Nielsen T,
657 Pons N, Levenez F, Yamada T, Mende DR, Li J, Xu J, Li S, Li D, Cao J,
658 Wang B, Liang H, Zheng H, Xie Y, Tap J, Lepage P, Bertalan M, Batto JM,
659 Hansen T, Le Paslier D, Linneberg A, Nielsen HB, Pelletier E, Renault P,
660 Sicheritz-Ponten T, Turner K, Zhu H, Yu C, Li S, Jian M, Zhou Y, Li Y,
661 Zhang X, Li S, Qin N, Yang H, Wang J, Brunak S, Dore J, Guarner F,
662 Kristiansen K, Pedersen O, Parkhill J, Weissenbach J, Meta HITC, Bork P,
663 Ehrlich SD, Wang J. A human gut microbial gene catalogue established by
664 metagenomic sequencing. *Nature* 2010;464(7285):59-65.
- 665 [37] Langmead B, Salzberg SL. Fast gapped-read alignment with Bowtie 2. *Nat*
666 *Methods* 2012;9(4):357-9.
- 667 [38] Truong DT, Franzosa EA, Tickle TL, Scholz M, Weingart G, Pasolli E, Tett A,
668 Huttenhower C, Segata N. MetaPhlan2 for enhanced metagenomic taxonomic
669 profiling. *Nat Methods* 2015;12(10):902-3.
- 670 [39] Franzosa EA, McIver LJ, Rahnvard G, Thompson LR, Schirmer M, Weingart
671 G, Lipson KS, Knight R, Caporaso JG, Segata N, Huttenhower C.
672 Species-level functional profiling of metagenomes and metatranscriptomes.
673 *Nat Methods* 2018;15(11):962-8.
- 674 [40] Buchfink B, Xie C, Huson DH. Fast and sensitive protein alignment using
675 DIAMOND. *Nature Methods* 2015;12(1):59-60.
- 676 [41] Markowitz VM, Chen IM, Palaniappan K, Chu K, Szeto E, Grechkin Y,
677 Ratner A, Jacob B, Huang J, Williams P, Huntemann M, Anderson I,
678 Mavromatis K, Ivanova NN, Kyrpides NC. IMG: the Integrated Microbial
679 Genomes database and comparative analysis system. *Nucleic Acids Res*
680 2012;40(Database issue):D115-22.
- 681 [42] Sievers F, Higgins DG. Clustal Omega, Accurate Alignment of Very Large
682 Numbers of Sequences. *Multiple Sequence Alignment Methods*
683 2014;1079:105-16.
- 684 [43] Johnson LS, Eddy SR, Portugaly E. Hidden Markov model speed heuristic and
685 iterative HMM search procedure. *Bmc Bioinformatics* 2010;11:431.

- 686 [44] Li DH, Liu CM, Luo RB, Sadakane K, Lam TW. MEGAHIT: an ultra-fast
687 single-node solution for large and complex metagenomics assembly via
688 succinct de Bruijn graph. *Bioinformatics* 2015;31(10):1674-6.
- 689 [45] Zhu WH, Lomsadze A, Borodovsky M. Ab initio gene identification in
690 metagenomic sequences. *Nucleic Acids Res* 2010;38(12):e132-32.
- 691 [46] Li W, Godzik A. Cd-hit: a fast program for clustering and comparing large
692 sets of protein or nucleotide sequences. *Bioinformatics* 2006;22(13):1658-9.
- 693 [47] Plaza Onate F, Le Chatelier E, Almeida M, Cervino ACL, Gauthier F,
694 Magoules F, Ehrlich SD, Pichaud M. MSPminer: abundance-based
695 reconstitution of microbial pan-genomes from shotgun metagenomic data.
696 *Bioinformatics* 2019;35(9):1544-52.
- 697 [48] Li H, Durbin R. Fast and accurate short read alignment with Burrows-Wheeler
698 transform. *Bioinformatics* 2009;25(14):1754-60.
- 699 [49] Bankevich A, Nurk S, Antipov D, Gurevich AA, Dvorkin M, Kulikov AS,
700 Lesin VM, Nikolenko SI, Pham S, Prjibelski AD, Pyshkin AV, Sirotkin AV,
701 Vyahhi N, Tesler G, Alekseyev MA, Pevzner PA. SPAdes: a new genome
702 assembly algorithm and its applications to single-cell sequencing. *J Comput*
703 *Biol* 2012;19(5):455-77.
- 704 [50] Zuo GH, Hao BL. CVTree3 Web Server for Whole-genome-based and
705 Alignment-free Prokaryotic Phylogeny and Taxonomy. *Genom Proteom*
706 *Bioinf* 2015;13(5):321-31.
- 707 [51] Friedman J, Alm EJ. Inferring correlation networks from genomic survey data.
708 *PLoS Comput Biol* 2012;8(9):e1002687.
- 709 [52] Shannon P, Markiel A, Ozier O, Baliga NS, Wang JT, Ramage D, Amin N,
710 Schwikowski B, Ideker T. Cytoscape: a software environment for integrated
711 models of biomolecular interaction networks. *Genome Res*
712 2003;13(11):2498-504.
- 713 [53] Wu DF, Jiao N, Zhu RX, Zhang YD, Gao WX, Fang S, Li YC, Cheng SJ, Tian
714 C, Lan P, Loomba R, Zhu LX. Identification of the keystone species in
715 non-alcoholic fatty liver disease by causal inference and dynamic intervention
716 modeling. *bioRxiv* 2020; doi: 10.1101/2020.08.06.240655.

717

718

719

Table1 Characteristics of the cohort included in this study

	Discovery cohort		Validation cohort	
	NAFLD	Control	NAFLD	Control
Sample Size	86	38	10	11
Age	51.56±12.67	55.71±12.75	53.7±3.65	56.18±6.65
BMI	30.25±5.46	23.03±1.88	34.1±1.2	23.19±0.92
Gender(F%/M%)	44.19/55.81	50.00/50.00	20.00/80.00	63.63/36.36
AST(U/L)	32.5±29.96	NA ^s	30.8±2.4	NA
LDL cholesterol(mg/dL)	116±37.12	NA	52.25±5.41 [#]	NA
HDL cholesterol (mg/dL)	46±15.97	NA	20.36±1.26	NA
Triglycerides(mg/dL)	129±95.70	NA	50.45±7.21	NA
Total cholesterol(mg/dL)	191.5±43.39	NA	95.90±5.41	NA

720

Data are presented as median±SD

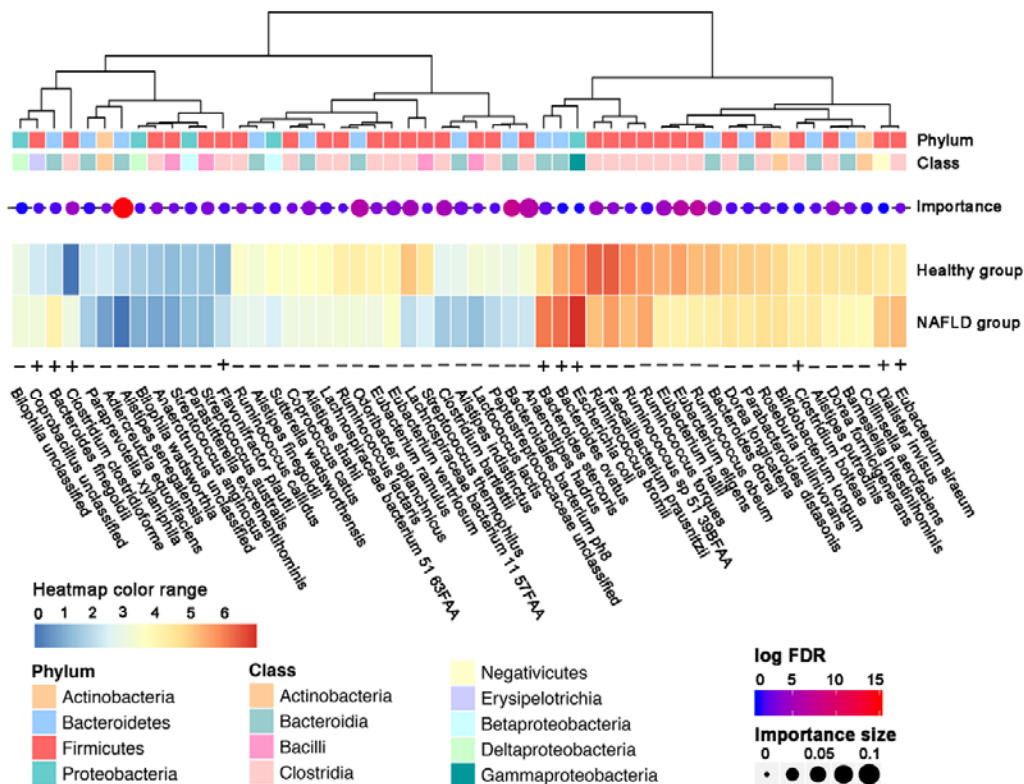
721

^s NA, not available. The control groups included healthy individuals (Ref 33 and 36)

722

[#] The data are converted from mmol/L to mg/dL.

723



724

725

Figure 1. The differential species distinguishing NAFLD patients from healthy

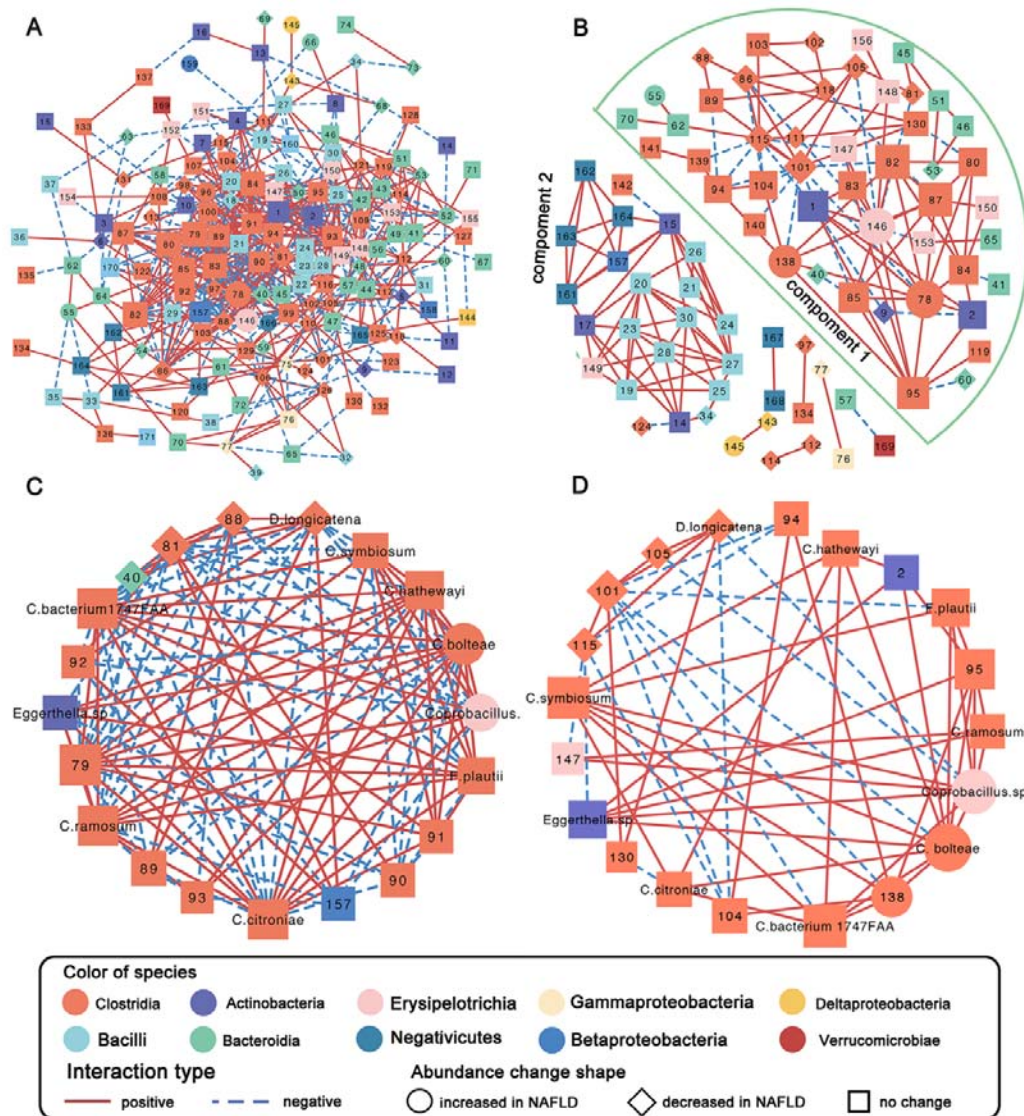
726

controls. Differential species were selected by statistical tests (two-tailed

727

Mann-Whitney U-tests adjusted by Benjamini–Hochberg). Furthermore, the

728 importance of the species that distinguish NAFLD patients from healthy controls was
 729 evaluated with random forest model. The heatmap shows the relative abundance
 730 (log-transformed) of the differential species in the NAFLD and the healthy groups,
 731 the size of the dots is proportional to the importance and the color shows the FDR
 732 value (-log-transformed). “+” indicates increased abundance while “-” indicates
 733 decreased abundance in NAFLD.



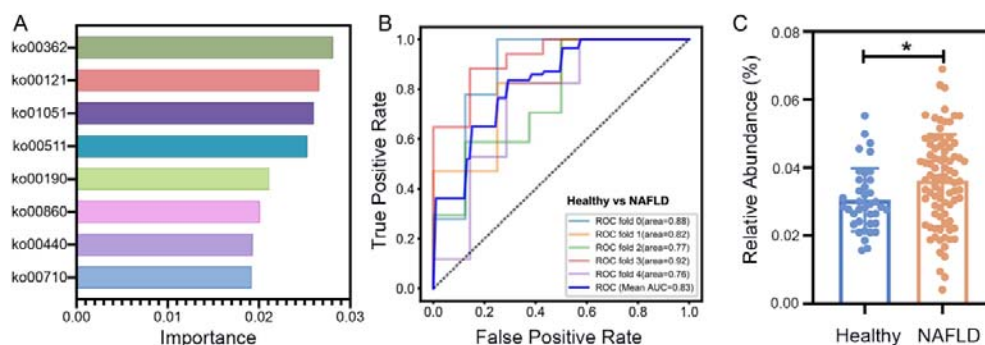
734

735 Figure 2. Microbiota “core community” in healthy controls (A&C) and NAFLD

736 patients (B&D). The microbial interactions were calculated using SparCC with 100

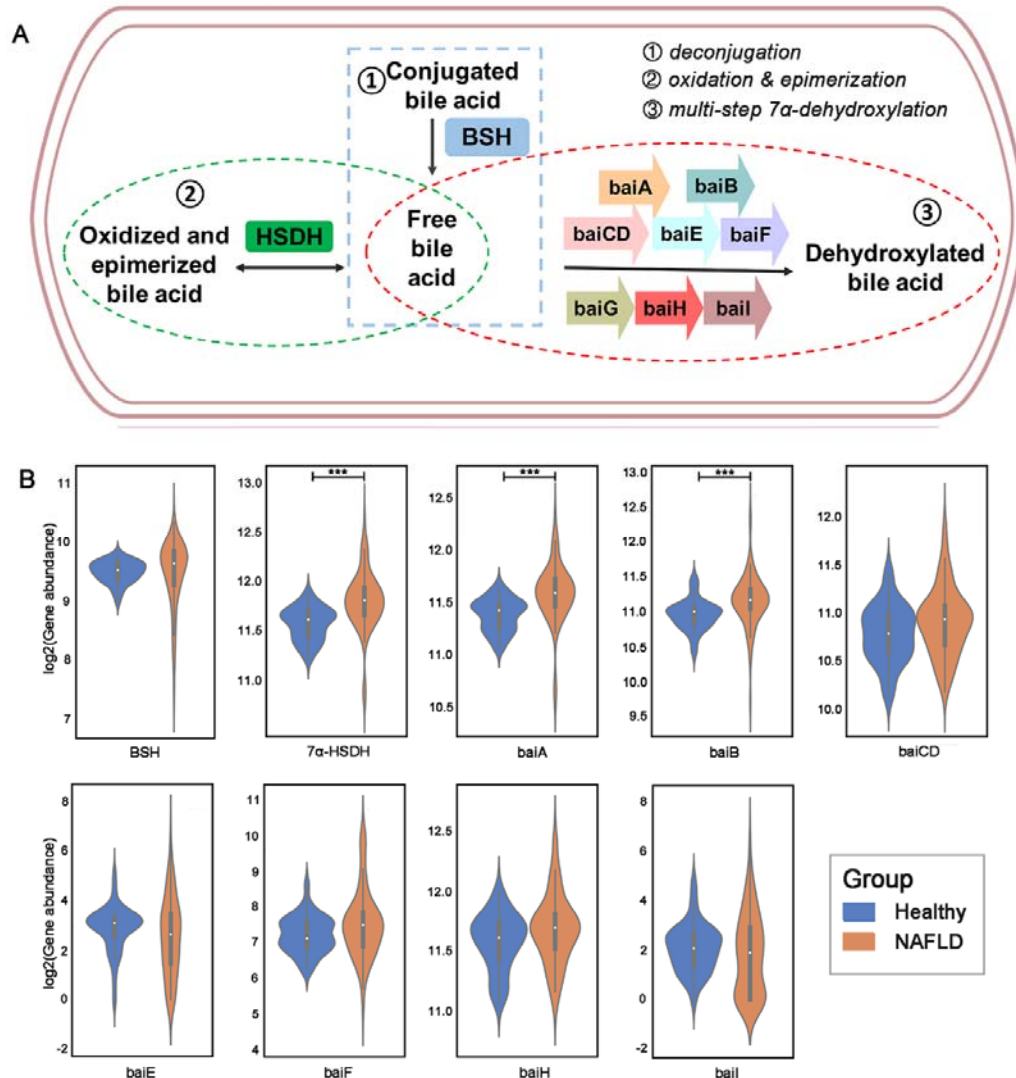
737 refining interactions, and p value of each interaction is approximated with 1000

738 permutations. Only interactions with p value < 0.05 and interactions with magnitudes
739 > 0.4 were included in the “core community”. The species were colored according to
740 the class they belong to and the node size indicates the hub score in their community.
741 Sub-network of top 20 hub nodes in healthy community (C) and NAFLD community
742 (D) was also plotted. The nodes indicated by species name were common species in
743 both sub-networks.



744

745 Figure 3. The differential pathway markers distinguishing NAFLD patients from
746 healthy controls. Differential pathways were selected by two-tailed Mann-Whitney U-
747 tests adjusted by Benjamini–Hochberg. Pathways with FDR values < 0.05 were
748 included. Important differential pathway markers were then identified with random
749 forest model and with the top 8 important pathways, the model achieved the highest
750 AUC value. (A). The importance of pathways evaluated in NAFLD with the random
751 forest model. (B). The AUC curve of random forest model with the top 8 important
752 pathways. (C). The abundance of secondary A biosynthesis pathway (ko00121) in the
753 healthy and the NAFLD groups. Values are the mean±SD. * indicates FDR<0.05.



754

755 Figure 4. The abundance of the bacterial genes related to secondary bile acid

756 synthesis. (A) Genes responsible for secondary bile acid biosynthesis can be grouped

757 into 3 categories: (1) deconjugation, (2) oxidation and epimerization and multi-step

758 7 α -dehydroxylation. (B) Gene abundance in health and NAFLD groups. Differences

759 were identified by two-tailed Mann-Whitney U- tests adjusted by

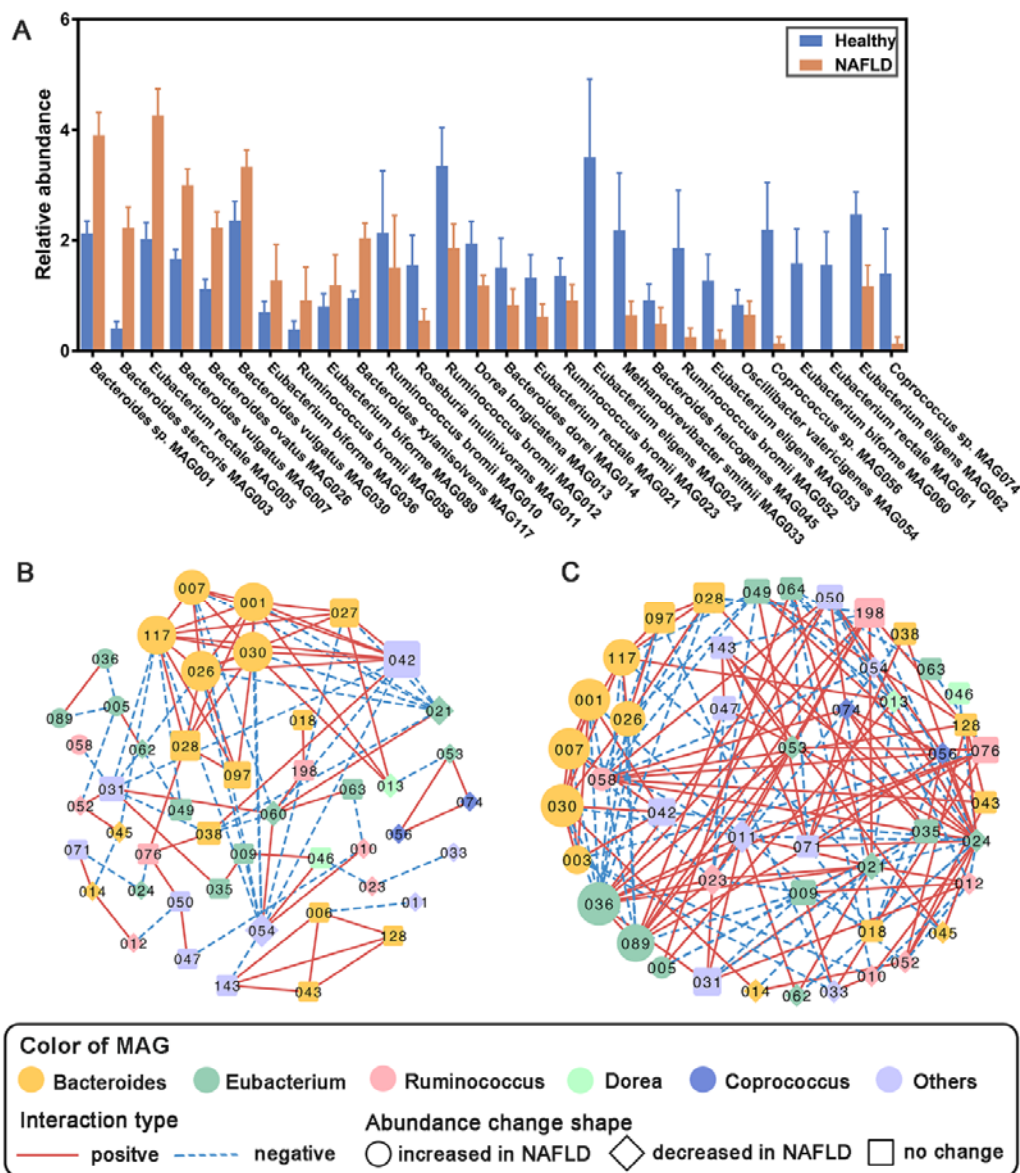
760 Benjamini–Hochberg. BSH: bile salt hydrolase; HSDH: hydroxysteroid

761 dehydrogenase; baiA, 3 α -hydroxysteroid dehydrogenase; baiB, bile acid-coenzyme A

762 ligase; baiCD, 7 α -hydroxy-3-oxo-D4-cholenoic acid oxidoreductase; baiE, bile acid

763 7 α - dehydratase; baiF, bile acid coenzyme A transferase/hydrolase; baiG, primary bile

764 acid transporter; baiH, 7beta-hydroxy-3-oxochol-24-oyl-CoA 4-desaturase; baiI, bile
 765 acid 7beta-dehydratase. *** indicates FDR<0.001.



766

767 Figure 5. BA metabolizing MAG in NAFLD and healthy subjects. (A) MAG

768 exhibiting differential abundance between healthy controls and NAFLD patients.

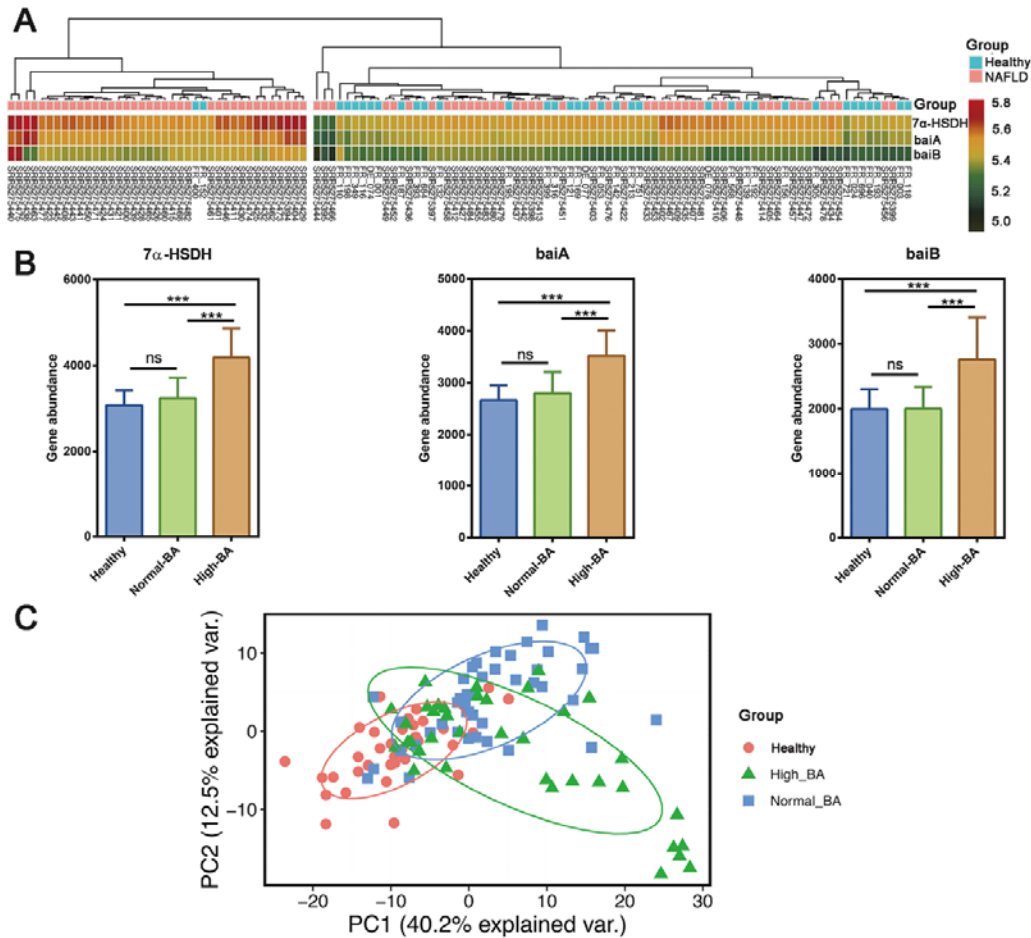
769 Differential MAG were selected by two-tailed Mann-Whitney U- tests adjusted by

770 Benjamini–Hochberg. MAG with FDR values < 0.1 were included. Values are mean

771 ± SEM. Interaction network for BA metabolising MAG community in healthy

772 controls (B) and NAFLD patients (C). Microbial interactions were calculated using

773 SparCC with 100 refining interactions, and p value of each interaction is
774 approximated with 1000 permutations. Only interactions with p value < 0.05 were
775 included.



776
777 Figure 6. Subgroups of NAFLD patients with different abundances of the secondary
778 BA synthesis genes. (A) NAFLD patients were clustered into two subgroups:
779 normal-BA subgroup and high-BA subgroup according to the abundances of 3
780 differential secondary BA synthesis genes. (B) Comparison of the abundances of 3
781 differential secondary BA synthesis genes among healthy control, normal-BA and
782 high BA groups. They were all significantly increased in high-BA subgroup, but was
783 not different between normal-BA subgroup and healthy group (Dunn tests adjusted by
784 Benjamini–Hochberg). (C) PCA plot based on the differential enzymes. Subjects were

785 clustered according to the secondary BA metabolizing potentials ($p < 0.001$ with
786 ANOSIM analysis). Values are mean \pm SD. *** indicates FDR $<$ 0.001.